CHINESE OPTICS LETTERS

Vol. 23, No. 1 | January 2025

# Divided GHz burst mode amplification to mJ burst energy and kHz burst rate

Yunfeng Wu (吴云峰)[1,2], Bowei Yang (杨伯威)[2], Zhe Lin (林 哲)[3], Ruoao Yang (杨若傲)[2], Xing Chen (陈 星)[3], Yanrong Song (宋晏蓉)[1], and Zhigang Zhang (张志刚)[2*]

[1] School of Physics and Optoelectronic Engineering, Beijing University of Technology, Beijing 100124, China

[2] State Key Laboratory of Advanced Optical Communication Systems and Networks, School of Electronics, Peking University, Beijing 100871, China

[3] State Key Laboratory of Information Photonics and Optical Communications, Beijing University of Posts and Telecommunications, Beijing 100876, China

*Corresponding author: zhgzhang@pku.edu.cn

Received April 14, 2024 | Accepted July 24, 2024 | Posted Online February 5, 2025

We demonstrated a divided pulse amplification of burst pulse trains. The intraburst rate is 1 GHz, and the burst rate ranges from 1.5 kHz to 15 MHz. Under the pump power of 100 W, the burst pulse energy is adjustable from 2.2 μJ to 22 mJ. The pulse width of combined and compressed pulses is 275 fs with beam quality $M^2$ of 1.2.

**Keywords:** burst-mode pulse; divided pulse amplification; high repetition rate fiber laser.
**DOI:** 10.3788/COL202523.011403

## 1. Introduction

Burst-mode pulses with high intrarepetition rates attract attention in many fields, such as ablation cooling[1,2], the generation of narrowband microwaves[3–5], and coherent pulse stacking[6–8]. For ablation-cooled micromachining, the intraburst pulse repetition rate ranges from 1 to 4 GHz; in the application of the pulse stacking, for shorter delay lines or cavities, the pulse repetition rate of 1 GHz is preferred[9,10] within the modulation bandwidth of electronics. Particularly, the burst-mode pulses could go around the limitation of nonlinearity, fully extracting the energy from the fiber amplifiers[11–14].

The key to burst pulse amplification is to generate the seed pulses with GHz intraburst repetition rate. There are a few methods, such as mode-locked lasers with GHz repetition rates[15–17] and continuous-wave (CW) lasers with high-speed modulation[3,4] where the direct generation with mode locking in a fundamental 1 GHz repetition rate is the most convenient. There have been quite a few reports on burst pulse amplifications. In the report of an average power of >100 W at an intraburst repetition rate of 1.2 GHz burst mode amplification, the pulses experienced four stages of the amplifier to boost the average power to 6.9 W before it was sent to the main amplifier[18,19]. However, the final pulse width is near 500 fs with a maximum burst energy of 800 nJ at a duty cycle of 10%. In a report of a "hybrid fiber amplification" combining chirped pulse amplification (CPA) and self-similar amplification[20], Ma *et al.* demonstrated the compressed of 35 fs with a pulse spectral width of 65 nm in a 1.02-GHz intraburst pulse rate. However, the individual pulse energy is only 110 nJ, in a 200-pulse burst, without sufficient pulse stretching. Another technique to produce burst-mode pulses is to modulate a CW laser with an electro-optic modulator. The intraburst repetition rate can be adjustable from 0.5 to 10 GHz, and the pulse duration is turned from 48 to 500 ps with 13 mJ burst pulse energy. However, because the pulses generated in this way have very little energy, the pulses have to experience more than five stages of amplifiers to boost the average power.

Previous reports on burst-mode amplification implied that, for a high intraburst pulse energy and a shorter pulse, a standard CPA system should be employed, which means the pulses must be stretched sufficiently and the stretcher dispersion must be paired with that of the compressor. A fast electro-optical modulator (EOM) for an individual pulse modulator is also required for even pulse energy.

In this Letter, we present a high-power divided burst-pulse amplification to 40 W. A burst pulse consists of 64 pulses with 1 ns time space (intraburst repetition of 1 GHz). Burst energy is 22 mJ when the burst rate is 1.5 kHz, where the single pulse energy is 340 μJ after compression. The pulse width is 275 fs without sidelobes.

## 2. System Setup

The schematic of the system is shown in Fig. 1. The system includes a seed pulse laser, 2 pre-amplifiers, and a power amplifier. As in a CPA, there are a pulse stretcher and a pulse compressor. There are also optical modulators for controlling the burst rate and the number of pulses in the burst. The seed pulse was generated in a 1 GHz fundamental repetition rate femtosecond fiber laser, which is similar to our previous study[15]. The

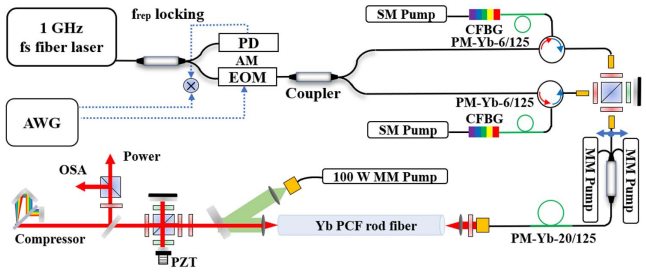


**Fig. 1.** Schematic of the divided burst-mode pulse amplification system. AM, amplitude modulation; SM, single mode; MM, multi mode; OSA, optical spectrum analyzer; PZT, piezoelectric ceramic; PD, photodiode.

repetition rate of the laser was locked to a microwave frequency of an arbitrary waveform generator (AWG), which controls the burst rate and intra-burst pulse number through an EOM as well.

The pulse train from the laser was trunked by the EOM into burst mode before the pulse stretching. This is because the EOM is much faster than acousto-optic modulators. A phase-locked loop was applied to keep the bias stable for sufficient contrast. The bandwidth of the EOM driver is 10 GHz. The burst rate is adjustable from 1.5 kHz to 15 MHz. To count against the gain saturation in the burst mode amplification, the intensity of the burst pulse train was also modulated in such a way that the pulses were equal-leveled after the power amplification.

In order to extract more single pulse energy in the burst without obvious nonlinear phase shift, we adopted the concept of "divided pulse amplification". The pulses were divided into two beams and coupled into two polarization axes to maintain fibers for independent amplifications. The first stage pre-amplifier was integrated with the pulse stretcher in such a way that the single mode polarization maintaining Yb:fiber (0.3 m each) was spliced between the circulators and the chirped fiber Bragg gratings (CFBGs), which allows the pump light to go through the tail of each CFBG into the gain fiber so that a wavelength division multiplexing (WDM) was saved. The seed pulses are amplified in round-trip before and after the stretcher, which makes the pre-amplifier compact and efficient.

The CFBGs are imprinted with a group delay dispersion and the third-order dispersion of 31.994 $ps^2$ and −0.354159 $ps^3$, respectively. The reflection bandwidth of the CFBG is 20 nm, which stretches the pulses to about 1.1 ns by calculation. It is noticed that the ratio of the third-order to second-order dispersion is 10 fs to ensure that they are simultaneously compensative by a grating pair by suitable incidence angle, including the dispersion of the fiber amplifier. We assumed that the CFBGs are identical in dispersion and reflection bandwidths. This has been proven by the pulse compression.

The pulses were combined again for the second stage amplifier which is a 0.6-m-long polarization maintaining (PM) double cladding fiber. The power amplifier is a rod-type large mode area and polarization maintaining photonic crystal fiber (PCF) which is a 0.8-m-long with a mode field diameter of 65 μm. The PCF was reversely pumped via a dichroic mirror to decrease the ASE.

Then the output pulses from the single PCF were collimated and combined again by a polarization beam splitter (PBS) and a delay line for compensating for the path delay in divided amplifiers.

The pulse compression was made by a transmission grating pair. The groove density of the compressor grating is 1739 line/mm. The grating incident angle was set to 59 deg to ensure that both the group delay dispersion (GDD) and the third order dispersion (TOD) are zero simultaneously including those in both CFBG and fiber amplifier.

## 3. Experimental Results

The output power of the 1 GHz femtosecond fiber laser was 320 mW under the total pump power of 1.3 W. The pulse width was 106 fs at a spectral bandwidth of 21 nm.

The single mode amplifier between the circulator and the CFBG compensated for the power losses in the modulation, and the power of each polarization was recovered to 300 mW before the cladding-fiber amplifier. The pre-amplifier boosted the power to 5 W pumped by two 8 W multi-mode diodes.

Before the main amplifier, the seed pulses have to be further prepared, including the burst repetition rate and the intensity of each pulse in the burst.

The output power curves of the main amplifier are shown in Fig. 2. The main amplifier boosted the burst pulse average power to more than 40 W at a pump power of 100 W at a weak dependence of the burst rate. It demonstrated that the low repetition rate burst mode could also fully extract the energy in the rod-type PCF, because of the long burst. Therefore, a burst pulse consists of $2^6 = 64$ pulses with 1 ns time space for subsequent pulse stacking, and the repetition rate of the burst was set to 1.5 kHz to obtain higher burst pulse energy.

For the burst-mode pulse amplification, one of the key issues is the gain saturation that makes the intra-burst pulse intensity descend in time. An intensity modulated was applied such that the seed pulses in the burst ascend in time, which makes the amplified pulse train equal in intensity. Figure 3(a) shows that

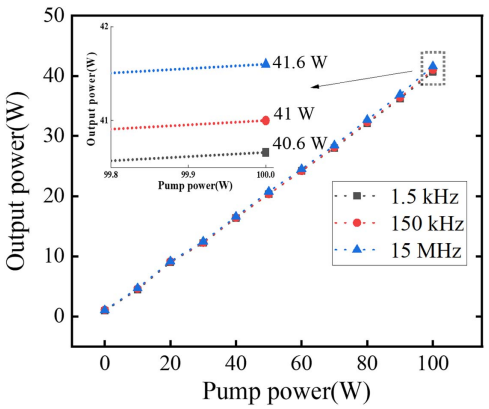


**Fig. 2.** The output power curves of the main amplifier at different repetition rates.

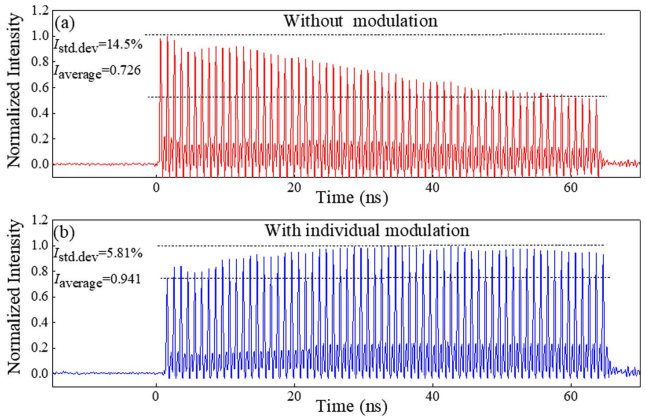


**Fig. 3.** The output amplified burst pulse trains (a) without intensity modulation; (b) with intensity modulation.

the train of the pulses in the burst continuously declines due to the gain saturation at a 100 W pump power. The intensity differs by 14.5% and the normalized average intensity is 0.726. By modulating the seed pulse intensity in a reversed profile, the output pulse train in the burst becomes nearly equal [Fig. 3(b)]. The normalized average intensity is 0.941.

The output power dependence on pump power in the main amplification for *s*- and *p*-polarized bursts are shown in Figs. 4(a) and 4(b). The average output powers are 19.43 and 19.72 W at a 100 W pump power, respectively.

The spectra of two polarized pulses are shown in Figs. 4(c) and 4(d). The central wavelength is 1032 nm with 10 nm 3 dB bandwidth for both *s*- and *p*-polarized pulses. Note that the spectra have a few modulation peaks, which might be mainly dominated by the self-phase modulation or cross phase modulation of different polarization stretches pulses.

The final *p*-polarized output power after pulse compression is 16.7 W, corresponding to the compressed efficiency of 86%.

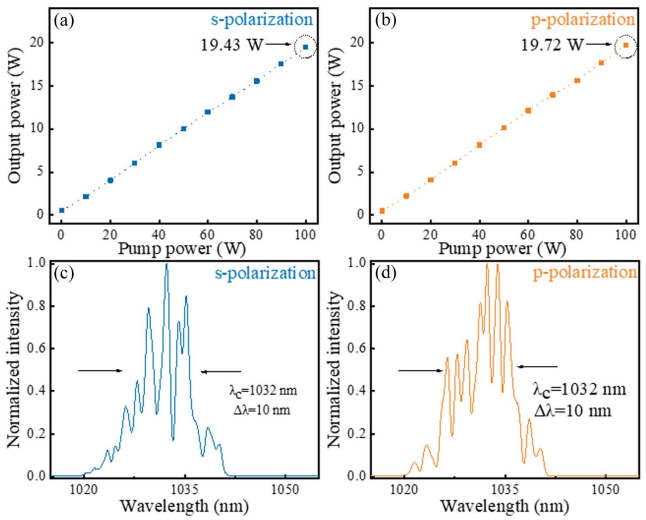


**Fig. 4.** The amplification results of two polarization pulses. (a) and (b) Output powers; (c) and (d) pulse spectra.

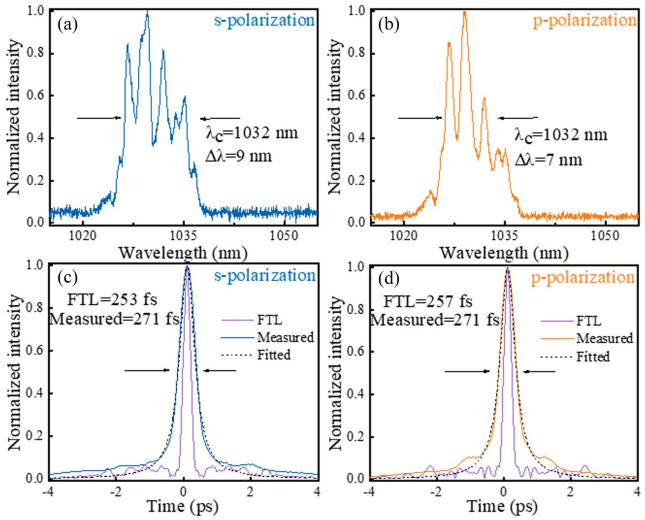


**Fig. 5.** The compression results of two polarization pulses. (a) and (b) Pulse spectra; (c) and (d) autocorrelation traces.

Then, the compressed pulses of two polarization pulses are independently measured, including spectra and autocorrelation traces, as illustrated in Fig. 5. The compressor filtered out low intensity modulation peaks on the sides of the spectrum, leading to spectral narrowing [Figs. 5(a) and 5(b)]. The pulse widths of Fourier transform-limited (FTL) traces are 253 and 257 fs, respectively, and the measured pulse duration is 271 fs without obvious pulse pedestals.

The two polarized pulse trains are then coherently combined with a delay line. The combined pulse spectrum and autocorrelation trace are shown in Fig. 6. There are similar modulation peaks in the pulse spectrum, but the spectral bandwidth becomes 10 nm due to gain narrowing [Fig. 6(a)]. The de-convoluted pulse is 275 fs with a little pedestal [Fig. 6(b)], which implies

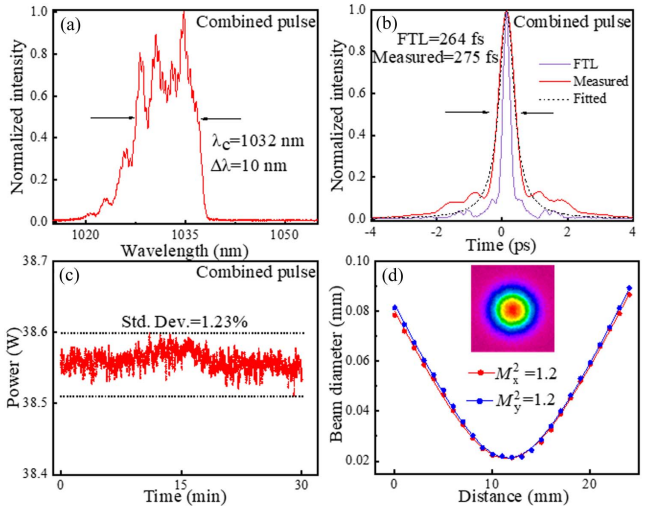


**Fig. 6.** Characteristics of the combined pulse. (a) Pulse spectrum; (b) autocorrelation trace; (c) power stability (before compressing); (d) $M^2$ measurement for both *x* and *y* axes.

the slightly different nonlinear phase between *s*- and *p*-polarized pulses. The output power of the combination pulse is 38.5 W, corresponding to the combination efficiency of 95%. The stability of output power was measured over 30 min. The standard deviation is 1.23% at 38.5 W (before compression), depicted in Fig. 6(c). Figure 6(d) shows the measured beam profile, indicating $M^2 = 1.2$ in both axes after combination. The calculated burst pulse energy was adjustable from 2.2 μJ to 22 mJ in the range of 15 MHz to 1.5 kHz burst rate.

## 4. Conclusions

We have demonstrated a divided pulse amplification of burst pulse trains in two polarizations over three-stage amplifiers. The seed pulse was divided into two polarizations and stretched and amplified individually in the first two stages. The two polarized pulse bursts were collinearly amplified in a PCF power amplifier and the output pulses were combined into one polarization.

The intra-burst rate is 1 GHz and the burst rate ranges from 1.5 kHz to 15 MHz. Under the pump power of 100 W, the amplified burst pulse energy is adjustable from 2.2 μJ to 22 mJ. The amplified pulse width is 275 fs. The measured beam quality of the combined beam is close to Gaussian beams. Further higher burst pulse energy can be expected to spatially combine more parallel amplifiers. The beam combination pulse stacking would become the key technique for high-power laser systems. Nevertheless, the high-power burst mode pulse amplification opens new ways for high throughput ablations as well as for pulse stacking.

## Acknowledgements

This work was supported by the National Natural Science Foundation of China (Nos. 61735001, 61575004, and 11027404).

## References

1. C. Kerse, H. Kalaycıoğlu, P. Elahi, *et al.*, "Ablation-cooled material removal with ultrafast bursts of pulses," Nature **537**, 84 (2016).
2. A. Nakamura, T. Mizuta, Y. Shimotsuma, *et al.*, "Picosecond burst pulse machining with temporal energy modulation [Invited]," Chin. Opt. Lett. **18**, 123801 (2020).
3. S. Liu, B. Zhang, Y. Bu, *et al.*, "High-energy and high-peak-power GHz burst-mode all-fiber laser with a uniform envelope and tunable intra-burst pulses,". High Power Laser Sci. Eng. **11**, e81 (2023).
4. X. He, B. Zhang, S. Liu, *et al.*, "High-power linear-polarization burst-mode all-fibre laser and generation of frequency-adjustable microwave signal," High Power Laser Sci. Eng. **9**, e13 (2021).
5. N. Ma, M. Chen, C. Yang, *et al.*, "High-efficiency 50 W burst-mode hundred picosecond green laser," High Power Laser Sci. Eng. **8**, e1 (2020).
6. S. Breitkopf, T. Eidam, A. Klenke, *et al.*, "A concept for multiterawatt fibre lasers based on coherent pulse stacking in passive cavities," Light Sci. Appl. **3**, e211 (2014).
7. H. Tünnermann and A. Shirakawa, "Delay line coherent pulse stacking," Opt. Lett. **42**, 4829 (2017).
8. S. Wang, J. Zheng, and J. Xu, "Phase-modulation-combination system for the generation of arbitrarily shaped repetition rate pulses," Chin. Opt. Lett. **11**, 030603 (2013).
9. T. Zhou, J. Ruppe, C. Zhu, *et al.*, "Coherent pulse stacking amplification using low-finesse Gires-Tournois interferometers," Opt. Express **23**, 7442 (2015).
10. B. Yang, G. Liu, A. Abulikemu, *et al.*, "Coherent stacking of 128 pulses from a GHz repetition rate femtosecond Yb:fiber laser," in *Conference on Lasers and Electro-Optics, OSA Technical Digest* (2020), paper JW2F.28.
11. Q. Zhao, G. Gao, Z. Cong, *et al.*, "High-repetition-rate, 50-μJ-level, 1064-nm, CPA laser system based on a single-stage double-pass Yb-doped rod-type fiber amplifier," Opt. Express **30**, 3611 (2022).
12. T. Luo, T. Wang, X. Pan, *et al.*, "396 MHz CPA femtosecond laser system based on a single crystal fiber rod-type amplifier," Appl. Opt. **62**, 8987 (2023).
13. R. Lü, H. Teng, J. Zhu, *et al.*, "High power Yb-fiber laser amplifier based on nonlinear chirped-pulse amplification at a repetition rate of 1 MHz," Chin. Opt. Lett. **19**, 091401 (2021).
14. Z. Zhao, H. Chen, Z. Zhang, *et al.*, "High peak power femtosecond cylindrical vector beams generation in a chirped-pulse amplification laser system," Chin. Opt. Lett. **20**, 031405 (2022).
15. C. Li, Y. Ma, X. Gao, *et al.*, "1 GHz repetition rate femtosecond Yb:fiber laser for direct generation of carrier-envelope offset frequency," Appl. Opt. **54**, 8350 (2015).
16. H. Chen, G. Chang, S. Xu, *et al.*, "3 GHz, fundamentally mode-locked, femtosecond Yb-fiber laser," Opt. Lett. **37**, 3522 (2012).
17. W. Wang, W. Lin, H. Cheng, *et al.*, "Gain-guided soliton: Scaling repetition rate of passively modelocked Yb-doped fiber lasers to 12.5 GHz," Opt. Express **27**, 10438 (2019).
18. Y. Liu, J. Wu, X. Wen, *et al.*, ">100 W GHz femtosecond burst mode all-fiber laser system at 1.0 μm," Opt. Express **28**, 13414 (2020).
19. H. Xiu, Y. Fan, W. Lin, *et al.*, "1200-W all polarization-maintaining fiber GHz-femtosecond-pulse laser with good beam quality," Opt. Express **31**, 41940 (2023).
20. J. Ma, H. Liu, Y. Chen, *et al.*, "Generation of 35 fs, 20 μJ, GHz pulse burst by hybrid fiber amplification technique," Opt. Express **31**, 34224 (2023).